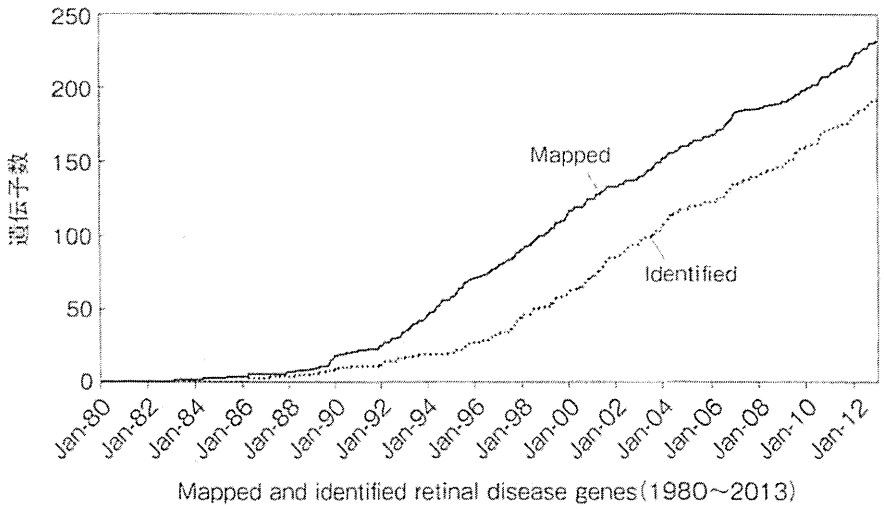


図 2　遺伝性網脈絡膜遺伝子の探索

RetNet(Daiger, S. P. et al.: Retinal Information Network. https://sph.uth.edu/retnet/home.htm)によって集計された遺伝性網脈絡膜疾患の遺伝子座がマッピングされた遺伝子数と，変異が発見された遺伝子数．この 15 年間，一定の傾きで増加しており，今後アジア人口の解析が進むことからさらに増加すると考えられる．

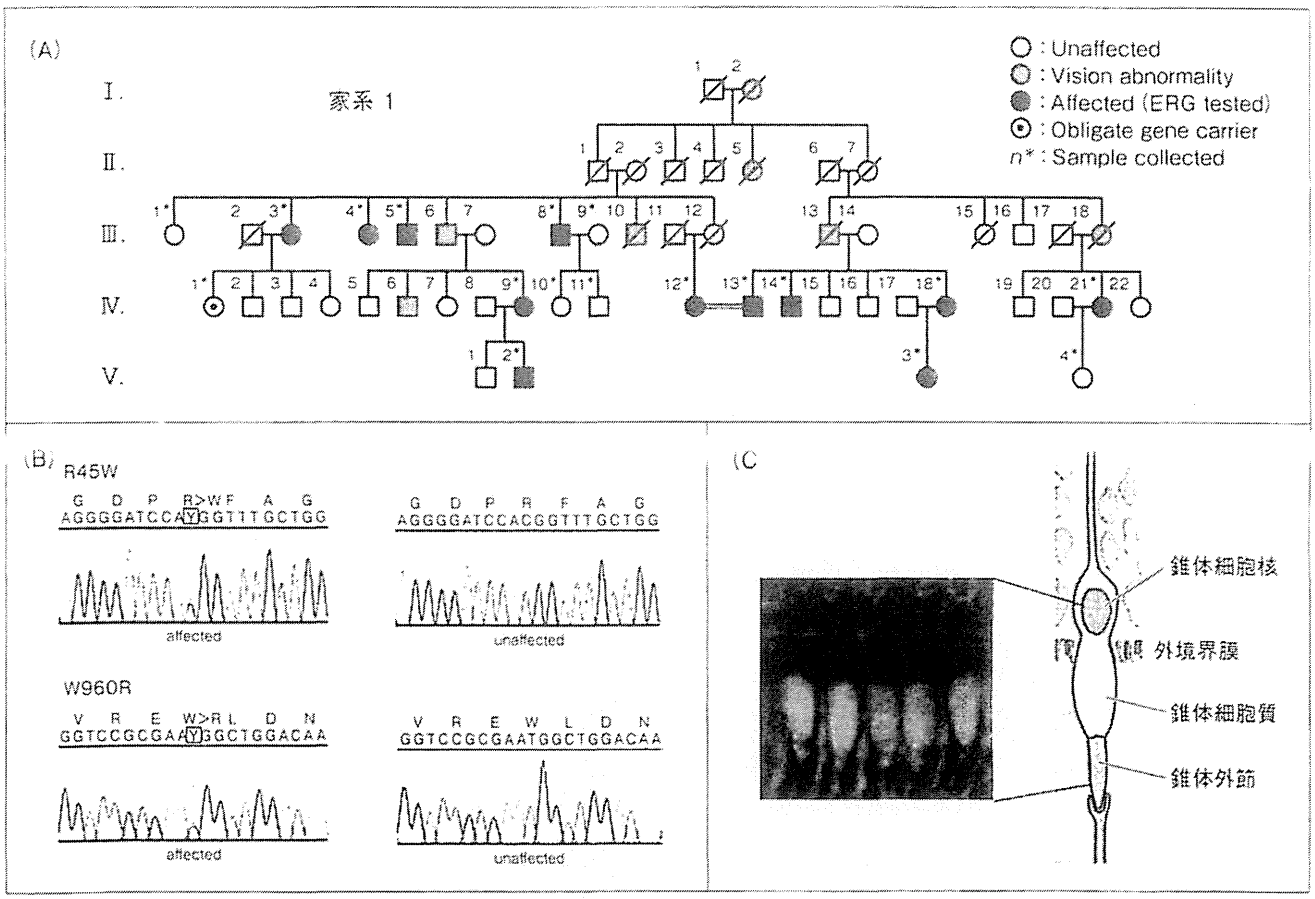


図 3　オカルト黄斑ジストロフィーとRP1L1遺伝子

A：オカルト黄斑ジストロフィーの家系．SNPHiTLink 連鎖解析法によって，8 番染色体短腕に疾患遺伝子がマッピングされた．

B：患者に観察された RP1L1R45W と W960R 遺伝子変異．

C：RP1L1 の免疫染色(緑)．RP1L1 の N 末端に対して作製された抗体によって視細胞の外境界膜から外節に染色が認められた．赤はロドプシンの免疫染色．桿体細胞の外節が染色されている．

な遺伝子解析が可能となった．これまでの解析結果から，すでに論文で報告されている欧米人の家系を対象とした既知原因遺伝子変異は約10～15%程度しか発見されておらず，日本人に特有の新規遺伝子変異が今後多数発見されることが期待されている．これらの遺伝子情報は韓国，中国，台湾，シンガポールなどの東南アジア諸国の遺伝子解析にも役立つ可能性があり，解析結果のアジア地域への情報発信が重要になると考える．最後に，遺伝子領域はゲノムのわずか1.6%しか占めておらず，残りの98.4%の非遺伝子領域の機能について重要な論文が報告されている[14]．遺伝子解析は非遺伝子領域をも研究対象とするステージに入っており，これらの研究成果が疾患の早期発見や予防に応用されることが期待される．

## 文献


1) Mitchell, G. A. et al.: *J. Clin. Invest.*, **81**：630-633, 1988.
2) Rosenfeld, P. J. et al.: *Nat. Genet.*, **1**：209-213, 1992.
3) Klein, R. J. et al.: *Science*, **308**：385-389, 2005.
4) Miyake, Y. et al.: *Am. J. Ophthal.*, **108**：292-299, 1989.
5) Fukuda, Y. et al.: *BMC Bioinformatics*, **10**：121, 2009.
6) Akahori, M. et al.: *Am. J. Hum. Genet.*, **87**：424-429, 2010.
7) Eckmiller, M. S.: *Prog. Retin. Eye Res.*, **23**：495-522, 2004.
8) Suzuki, H. et al.: *Nat. Genet.*, **41**：553-562, 2009.
9) Zeitz, C. et al.: *Am. J. Hum. Genet.*, **92**：67-75, 2013.
10) Audo, I. et al.: *Am. J. Hum. Genet.*, **90**：321-330, 2012.
11) Ozgül, R. K. et al.: *Am. J. Hum. Genet.*, **89**：253-264, 2011.
12) Tucker, B. A. et al.: *Proc. Natl. Acad. Sci. USA*, **108**：E569-E576, 2011.
13) Otto, E. A. et al.: *Nat. Genet.*, **42**：840-850, 2010.
14) The ENCODE Project Consortium：*Nature*, **486**：57-74, 2012.


*　　*　　*

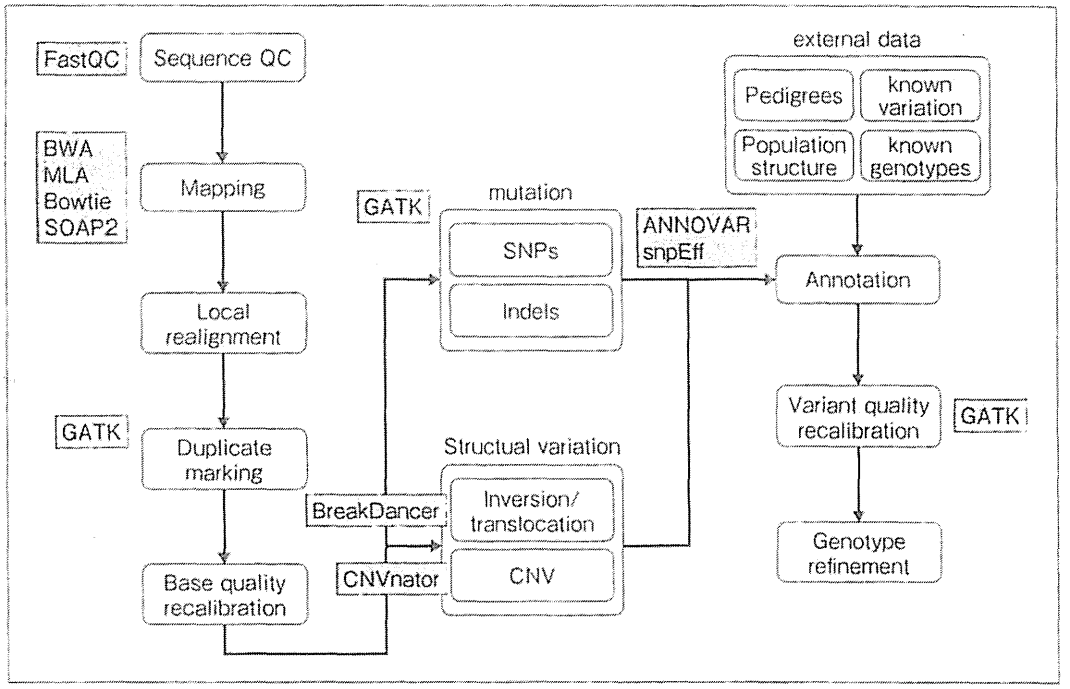


図 5　エクソームデータ解析のフロー

Re-sequencing による原因変異同定のための解析フロー．配列データのクオリティチェックからマッピング，コーリング，アノテーションまでの流れを示している．グレーに色づけられているのはそれぞれの処理に用いられるプログラムの名前である．

詳細な情報は http://cell-innovation.nig.ac.jp/ からも提供している．また，実際の解析パイプラインの実行も可能である．

はじまる．マッピングを行うために，著者らは BWA(Burrows-Wheeler Aligner)をおもに用いている．つぎに，参照ゲノムにマッピングされたエクソーム配列からサンプルのエクソン配列を再構築し，GATK(Genome Analysis Toolkit)を用いて挿入・欠失を含めた SNV の同定(コーリング)を行う．得られた変異情報は snpEff や Annover を用いてアノテーション情報が付加される．また，対象疾患に関連しない既知変異の除去や変異のパターンによってアミノ酸を変える非相同性置換や変えない相同性置換などの情報や種間での保存を考慮した情報量をもとに，機能に対する影響度を考慮して原因変異の同定を行う．

この際一番大事なのは，得られた SNP 情報からいかに効率よくかつ精度高く原因変異を抽出するかである．このために既知変異情報を用いたフィルタリングが有効である．この目的でよく使われるのが dbSNP のデータである．これはアメリカが中心となり世界中のさまざまな人種 1,000 人のゲノム配列の決定を行ったプロジェクトのデータを含んだ SNP 情報データベースである．このデータベース情報を用いることにより，既知変異や疾患に関連のない変異情報を取り除くことができる．

しかし，実際のデータを解析する場合には，これだけでかならずしもうまくいかないのも事実である．実際には家族サンプルや近親婚サンプルなどを使用してより精度の高い推定を行うことが行われている．さらに，対象としている疾患が浸透率 100%でない，表現型の定義が不十分であるなどにより，原因変異の同定が困難になることもある．また，エクソーム解析の弱点であるが，原因変異がエクソン以外の場所にあることもある．

## おわりに

近年の革新的な DNA シークエンス技術の進歩によって，全ゲノム配列を解読することを視野に入れた眼疾患の原因遺伝子探索が盛んになっている．アメリカを中心に，この技術を利用した遺伝性網脈絡膜疾患の新規原因遺伝子が複数報告されている[9-13]．われわれは日本人患者とその親族のエクソーム解析によって，これまで十分な解析が行われていなかった遺伝性網脈絡膜疾患の網羅的

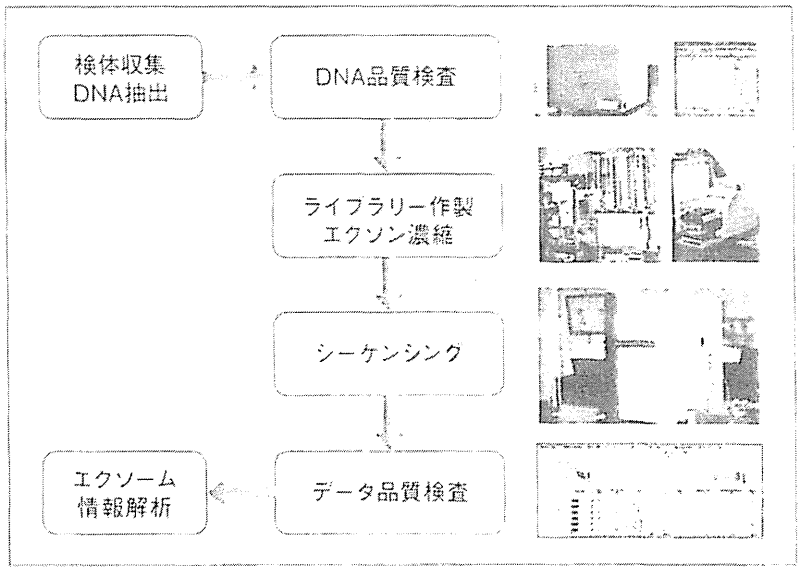


**図 4　エクソーム解析の流れ**

遺伝性網膜疾患家系より収集された検体について，DNA 品質検査，ライブラリー作製・エクソン濃縮，シーケンシング，およびデータ品質検査のプロセスを実行している．これらのプロセスにより得られたデータを用いて，疾患の原因変異を同定するための情報解析が行われる．

プット化とライブラリー品質の安定化を実現している．塩基配列解析にはイルミナ社 HiSeq2000 シーケンサーを用いている．

ライブラリー作製時にインデックス配列を付加することにより多検体のライブラリーを混合し，同時にシーケンシング解析することが可能である．たとえば，一度のランで 50 検体の同時解析を行うことで，1 検体当り約 10GB の塩基配列データ（ターゲットエクソン領域の約 140 倍に相当）を得ることが可能である．得られた塩基配列データについては，検体当りの有効リード数やゲノムへのマッピング率など，エクソーム情報の解析に必要な品質を満たしていることを確認している．これらのプロセスは理研 OSC にて構築したプロジェクトの情報と進捗を記録するための LIMS（LS-archive）を用いて管理している．LS-archive にはプロジェクトの基本情報，サンプル情報，ライブラリー解析，シーケンス解析，データ解析の情報および各プロセスの実行状況が記録される．これらの情報は表やグラフにより視覚的に表示され，研究者がプロジェクトの進捗状況や品質を容易に把握することができる．

## エクソーム解析

全エクソーム解析（WXS）は，全ゲノム配列のなかの蛋白質をコードするエクソンのみに焦点を当てている．当然，全ゲノム領域を対象とした全ゲノムシークエンスのほうがより多くの情報量が期待されるが，エクソン領域は全ゲノム領域の 1～1.5%であり，シークエンスおよびデータ解析に関するコストや時間が大幅に削減されるうえに，蛋白質配列に影響を与える重要な変異の情報を網羅的に得ることができる．エクソームを用いることにより蛋白質配列変異と疾患などの表現型の関連が明らかになることが期待される．この方法はまれな Mendel 遺伝疾患の原因遺伝子の探索で成果を収めており，さらに，より複雑な遺伝疾患の研究にも対象が広げられている．

具体的にエクソーム解析を行う場合についてデータ解析のプロセスを説明する（図 5）．最初に得られた配列データからクオリティの低いものを除去する．これは後の解析において擬陽性を排除するために大事なプロセスである．つぎに，エクソームデータの場合にはすでに参照できるゲノム配列データがあることが前提であるので，まず得られたエクソーム配列を対照としてのリファレンスゲノムに貼り付けていく（マッピング）ことから

患もあるが，そのなかでも世界的に有病率の高い難病に加齢黄斑変性がある．アメリカでは中途失明の原因として第一位であり，日本でも急速な高齢化によって患者数が増加している．加齢黄斑変性は遺伝子，加齢，喫煙，肥満，青色光など複数の要因によって発症することが疫学調査によって明らかにされており，この10年間に発症機序が徐々に明らかになってきた．多因子疾患として全ゲノム相関解析が行われ，医学分野では初めての感受性遺伝子，補体H因子(complement factor H)が発見されている[3]．

## オカルト黄斑ジストロフィー(三宅病)

黄斑ジストロフィーの一種で，黄斑部の錐体機能のみが著しく低下するMendel優先遺伝形式のオカルト黄斑ジストロフィー(occult macular dystrophy：OMD)は日本人眼科医によって発見された数少ない眼疾患のひとつで[4]，著者らによってその原因遺伝子が解明された．著者らは佐渡で発見されたOMDの大家系からDNA検体を収集し，SNPチップを用いた新しい連鎖解析法(SNP HiTLink)[5]を用いて解析を行った(図3)．その結果，染色体8番短腕にLOD Score 3.7以上の高い連鎖が発見され，この連鎖不平衡の約10MBの領域に絞り込まれた．この領域には少なくとも128遺伝子が存在し，網膜で発現する22の遺伝子が抽出された．

さらに，各遺伝子の文献やデータベースによる情報から4つの遺伝子候補が選択され，ダイレクトシークエンスによって，*RP1L1*(R45W)遺伝子変異が発見された[6]．*RP1L1*は網膜色素変性の原因遺伝子RP1に類似する遺伝子としてクローニングされ，当初は多くの患者がスクリーニングされたが，遺伝子変異は発見されず，今回黄斑ジストロフィーの原因遺伝子変異として検出された．

ヒトRP1L1蛋白質に対して作製された抗体を用いてカニクイザルの網膜切片について免疫染色を行った結果，視細胞の外節と細胞体をつなぐ微小管(connecting cilia)に特異的な染色が観察された．視細胞の微小管は高度に分化しており，細胞体と外節の間の輸送機能を担うと同時に，視細胞を光軸に沿って細胞の傾きを修正する機能がある[7]．この機能が阻害されると中心窩の錐体細胞は光軸に対して斜め方向に傾き，感光性は著しく低下する可能性がある．また，錐体細胞はエネルギー消費量が桿体細胞に比べて大きいことから，変異によって微小管の機能が阻害され，細胞輸送がもっとも盛んな中心窩において錐体細胞が十分に機能していない可能性もある．RP1L1はRP1蛋白質と相互作用することが明らかにされており，RP1が微小管の機能に関与していることからRP1L1も同様な機能があると考えられる．RP1の遺伝子変異によるOMDの発症について現在調査されている．

## 遺伝性網膜疾患のエクソームシークエンス

次世代シーケンサーによる全エクソン塩基配列解析技術により，家族単位で罹患者および親族のDNA検体を比較することによって，疾患の原因となる遺伝子変異を効率よく発見することが可能となった．著者らは，東京医療センターおよび関連病院で遺伝性網脈絡膜疾患の臨床診断と検体の収集を行っている．網膜疾患の臨床診断にあたっては電気生理学的検査を含む視機能検査を包括的に実施し，家系情報，症例情報(眼底所見，螢光眼底造影，網膜電図)がオンライン症例登録システムを用いて東京医療センターで収集されている．

患者および親族から採取した血液より抽出したゲノムDNAのエクソームシークエンス解析は，理化学研究所オミックス基盤研究領域(理研OSC)にて行われている．理研OSCでは次世代シーケンサーを早期から導入し，独自のライブラリー作製技術および大規模塩基配列解析技術を用いたライフサイエンス研究を展開してきた[8]．これらの施設と技術基盤を活用し，図4に示したプロセスに従ってエクソーム塩基配列解析を行っている．DNA品質検査プロセスでは収集されたDNA検体について吸光度測定，PicoGreenによる二本鎖DNA濃度定量を実施し，つぎに超音波破砕装置コバリスによる断片化およびアジレント社SureSelectキットを用いたライブラリー作製，エクソン濃縮を行う．このプロセスには最大96サンプルの同時処理が可能なアジレント社の自動ライブラリー作製システムを導入しており，ハイスルー

第39巻第3号平成25年3月25日発行（毎月1回25日発行）　昭和54年8月27日第3種郵便物認可
ISSN 1347-4340

# Medical Science Digest

# MSD

Vol.39
No.3
2013
通巻506号

3

メディカル・サイエンス・ダイジェスト

## 特集 アンチエイジングと疾患

特集編輯 森下　竜一
（大阪大学臨床遺伝子治療学）



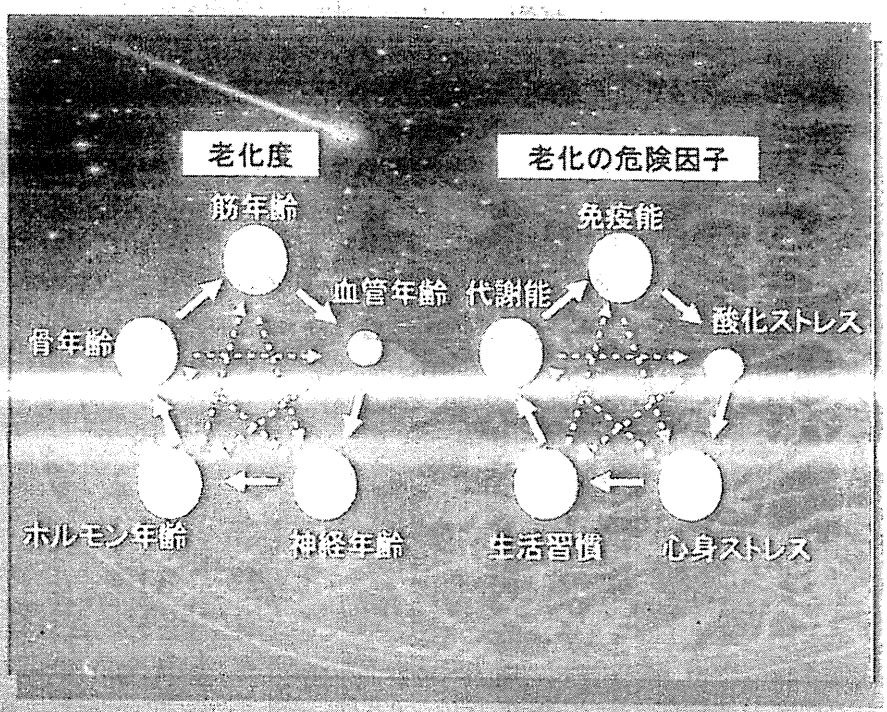






ニューサイエンス社

MSD Medical Science Digest
メディカル・サイエンス・ダイジェスト
Vol.39 No3 2013
3月号

目次

# 特集　アンチエイジングと疾患

What is Anti-Aging Medicine ?

特集編輯　森下　竜一



表紙写真の解説

アンチエイジング治療の原則は，病気になる前に，老化度や老化の危険因子を判定し，弱点の是正や改善に努めることである。図は，老化度や老化危険因子の各指標を知るしており，このバランスが崩れると病気が発症する。

(表紙図提供・解説：大阪大学大学院医学系研究科臨床遺伝子治療学　森下竜一)

Digest シリーズ

—新規原因遺伝子Optineurin—　Vol.5(完)

# Optineurinと正常眼圧緑内障

Optineurin and glaucoma

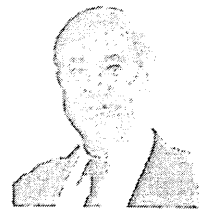

岩田　岳（いわた　たけし）
1988年名城大学大学院農学研究科博士課程卒業。'88年National Eye Institute, NIH留学。2004年（独）国立病院機構東京医療センター臨床研究センター室長，'07年同 部長。研究テーマ：遺伝性網膜疾患，緑内障，加齢黄斑変性

岩田　岳

独立行政法人国立病院機構東京医療センター
臨床研究センター（感覚器センター）
分子細胞生物学研究部

Key Words: Optineurin, Rab8, Normal tension glaucoma

## はじめに

緑内障は視神経の中でも神経節細胞死を主な特徴とする眼疾患で，周辺視野から視野欠損が進行する。日本人における失明原因で最も有病率が高い眼疾患であり，その原因解明と進行予防の薬物開発が進んでいるが根本治癒には至っていない。緑内障は病理学的に開放隅角緑内障，閉塞隅角緑内障そして発達緑内障に分類され，その中でも開放隅角緑内障が最も患者数が多い。緑内障は眼圧の上昇をともなう場合とともなわない場合があり，日本人には後者が多いことが，岐阜県多治見市で行われた疫学的調査[1]によって明らかにされている。眼圧上昇は眼球前房を循環する房水の流出路にあたる線維柱帯やその背後にあるシュレム管の障害によって流出抵抗が増加することによって眼内圧力が高まると予想され，この圧力上昇は眼球後極の視神経に機械的なストレスを与える。

緑内障は多因子疾患と考えられており，加齢にともなう機能低下によって発症頻度は上昇するが，その病態機序は未だ不明である。遺伝要因の重要性が強調されてきたが，ゲノム相関解析などでも特定の遺伝子変異を発見するには至っていない。このような状況において，低い頻度ではあるが，高いオッズ比で緑内障を誘発する少数の遺伝子変異が明らかにされている。この中でも高眼圧の開放隅角緑内障の原因遺伝子としてミオシリン（Myocilin）と正常眼圧緑内障の原因遺伝子としてオプチニュリン（Optineurin）が複数の研究グループによって確認されている。これらは緑内障の分子メカニズムを解明する数少ない手掛かりとして，精力的に研究されている。

## 緑内障原因遺伝子オプチニュリンの発見

正常眼圧緑内障の家系について連鎖解析が行われ，その原因遺伝子の遺伝子座が染色体10p15-p14（*GLC1E*）に存在することが明らかになり[2]後にこの領域にOptic Neuropathy Inducing Protein，オプチニュリン（Optineurin, *OPTN*）が発見された[3]。この最初の論文で調査された開放隅角緑内障の約16%の家系においてオプチニュリンの遺伝子変異が発見されたと報告されたが，世界的な検証によってその多くは遺伝子多型として検出され，現在ではGlu50Lys(E50K)が唯一緑内障の原因遺伝子変異として認知されている。この遺伝子変異によっ

Takeshi Iwata
National Hospital Organization Tokyo Medical Center
National Institute of Sensory Organs, Division of Molecular & Cellular Biology

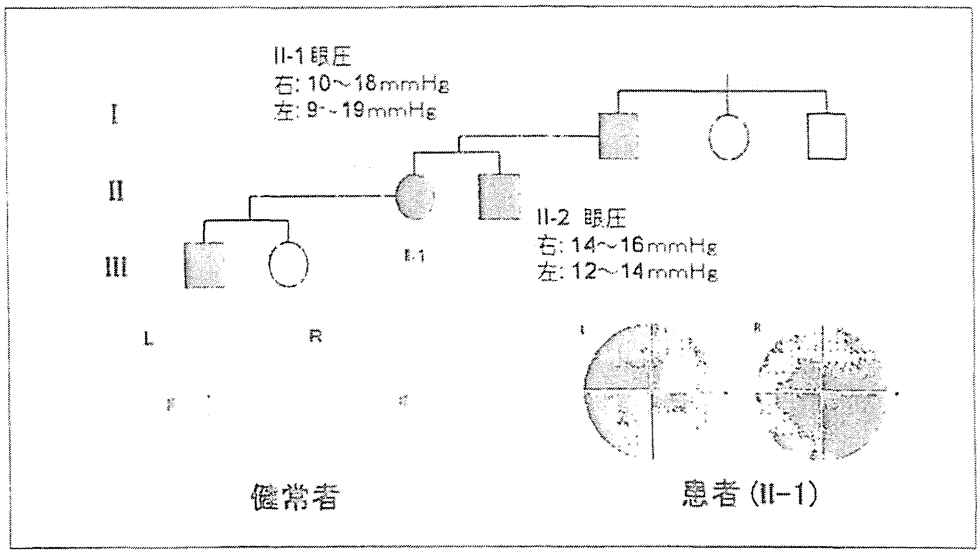


図1　オプチニュリンE50Kが検出された正常眼圧緑内障の家系図と視野検査
黒塗り患者，白塗り健常者（岐阜大学医学部眼科学教室　山本哲也教授，川瀬和秀准教授より情報提供[4]）

て重篤な正常眼圧緑内障を発症する家系が岐阜大学眼科学教室の山本哲也教授，川瀬和秀准教授によって発見され（図1），この家系の10代，40代，70代のそれぞれの患者を診断することによって，視野欠損が進行することが明らかにされた[4]。また船山，布施らによって日本人緑内障患者においてH26Dの遺伝子変異も報告されている[5]。

## 緑内障に関係するオプチニュリンの機能

オプチニュリンタンパク質は577アミノ酸から構成され，多くの細胞で発現している。オプチニュリンは複数のタンパク質と相互作用することが知られており，Rab8，ハンチントン，ミオシンVIなど，細胞内のゴルジ体から細胞膜外への分泌機能に関わっていると考えられる。細胞内でのオプチニュリンの欠損によって小胞体の分解が促されるとの報告がある(RD 2012, Bavaria, Germany)。E50Kが位置するタンパク質のN末端よりの部分はbZIP構造になっており，Rab8の結合部位に近いことから，E50K変異によって，オプチニュリンとRab8との相互作用が障害されると考えた筆者らは，これを証明するために分子間相互作用やE50Kを高発現するトランスジェニックマウスを作製して，これを証明した[6]（図2）。

さらに，高眼圧の緑内障遺伝子ミオシリンとオプチニュリンは相互作用するとの報告があり，これらの緑内障タンパク質は同じパスウエイに関係することが示唆されている。全ゲノム相関解析によってアポリポタンパク質(ApoE) 遺伝子のプロモーター領域 (-219G)に発見された遺伝子多型は視神経乳頭の障害と強く相関しており，さらにApoE遺伝子はModifier GeneとしてミオシリンのTransgenic活性に作用して，高眼圧の開放隅角緑内障を発症させるとの報告もある。Modifier Geneとは他の遺伝子に影響力を持つ遺伝子であり[7]，同様な関係か

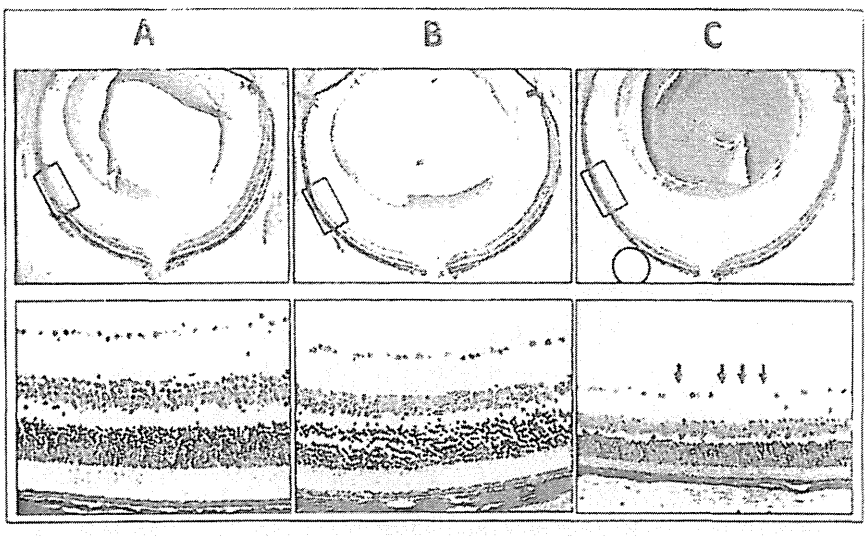


図2　オプチニュリンE50K変異体を発現するトランスジェニックマウスの眼球切片
網膜の周辺域で視神経の委縮が観察された。A：正常マウス，B：野生型オプチニュリントランスジェニックマウス，C：E50K変異体オプチニュリントランスジェニックマウス[10] 周辺網膜の委縮が観察される。

TNF-αとオプチニュリンの遺伝子多型についても報告されている[6]。

## オプチニュリン変異体を発現する緑内障モデル動物の開発

緑内障研究においてモデル動物の存在はきわめて重要な存在である。モデル動物を使って隅角や視神経網膜における進行を経時的に観察することや薬効評価に利用できることが求められる。これまでにも自然発症のイヌや隅角の外科的手術による霊長類モデル動物が報告されてきた。緑内障の原因遺伝子の解析には遺伝子改変に適するマウスが，広く使われているが，マウスとヒトでは眼球サイズが大きく異なり，神経乳頭周辺の血管構造が異なることや，篩状板が存在しないなどの違いがあり，その取り扱いや実験結果の解釈が難しい。マウスの系統によっては10から20 mmHgの眼圧差が存在することも知られている。緑内障遺伝子としてはオプチニュリンとミオシリン等の遺伝子改変マウスが作製され，緑内障の発症機序解明の研究に利用されている。

我々が作製したオプチニュリンE50K変異体を発現したマウスでは，正常眼圧が維持されたまま，生後1年で網膜神経節細胞死や視神経乳頭の陥凹が観察されている[4]。視神経の障害は網膜周辺から徐々に中央へと進行することが観察されている。さらにグリア細胞の活性化による周辺神経細胞への影響や血流障害の可能性が示唆された。このマウスに対比されるのが，ミオシリンTyr437His変異を発現する眼圧上昇型のトランスジェニックマウスである。このマウスは正常マウスに比べて昼は2 mmHg，夜は4 mmHgの眼圧上昇が認められ，生後1年目には網膜神経節細胞数の20%が減少する[7]。

## おわりに

緑内障の病態機序に関する情報が限られる状況において，オプチニュリン遺伝子変異による正常眼圧緑内障の発症は世界中の眼科研究者を引き付けている。E50Kトランスジェニックマウスによってオプチニュリンの変異体が網膜内のどの細胞にストレスとなっているか明らかになってきた。さらにオプチニュリンが関わる小胞顆粒の輸送について，どのような生体分子の分泌に関わっているのか明らかにされることによって，この生体分子が正常眼圧緑内障の薬としても開発される可能性もある。日本人には家族性の緑内障が多く存在することが知られており，次世代型DNAシークエンサーの登場により，これらの原因を明らかにする研究プロジェクトが日本で進行しており，その成果が期待されている。

### 文　献


1) Iwase A, Suzuki Y, Araie M, *et al.* Tajimi Study Group, Japan Glaucoma Society. The prevalence of primary open-angle glaucoma in Japanese: the Tajimi Study. Ophthalmology 2004; 111: 1641-8.
2) Sarfarazi M, Child A, Stoilova D, *et al.* Localization of the fourth locus (GLC1E) for adult-onset primary open-angle glaucoma to the 10p15-p14 region. Am J Hum Genet 1998; 62: 641-52.
3) Rezaie T, Child A, Hitchings R, *et al.* Adult-onset primary open-angle glaucoma caused by mutations in optineurin. Science 2002; 295: 1077-9.
4) Chi Z-L, Akahori, A, Obazawa M, *et al.* Overexpression of optineurin E50K disrupts Rab8 interaction and leads to a progressive retinal degeneration in mice. Hum Mol Genet 2010;19 : 2605-15.
5) Copin B, Brézin AP, Valtot F, *et al.* Apolipoprotein E promoter singlenucleotide polymorphisms affect the phenotype of primary open angle glaucoma and demonstrate interaction with the myocilin gene. Am J Hum Genet 2002; 70: 1575-81.
6) Funayama T, Ishikawa K, Ohtake Y, *et al.* Variants in optineurin gene and their association with tumor necrosis factor-alpha polymorphisms in Japanese patients with glaucoma. Invest Ophthalmol Vis Sci 2004; 45: 4359-67.
7) Senatorov VV, Malyukova I, Fariss R, *et al.* Expression of mutated mouse myocilin induces open-angle glaucoma in transgenic mice. J. Neurosci. 2006; 26: 11903-14.

HMG Advance Access published May 21, 2013

*Human Molecular Genetics, 2013* 1–9
*doi:10.1093/hmg/ddt210*

# Enhanced optineurin E50K–TBK1 interaction evokes protein insolubility and initiates familial primary open-angle glaucoma

**Yuriko Minegishi[1], Daisuke Iejima[1], Hiroaki Kobayashi[1], Zai-Long Chi[1], Kazuhide Kawase[2], Tetsuya Yamamoto[2], Tomohisa Seki[3], Shinsuke Yuasa[3], Keiichi Fukuda[3] and Takeshi Iwata[1,*]**

[1]Division of Molecular and Cellular Biology, National Institute of Sensory Organs, National Hospital Organization Tokyo Medical Center, Tokyo, Japan [2]Department of Ophthalmology, Gifu University School of Medicine, Gifu, Japan [3]Department of Cardiology, Keio University School of Medicine, Tokyo, Japan

Received March 13, 2013; Revised April 15, 2013; Accepted May 1, 2013

**Glaucoma is the leading cause for blindness affecting 60 million people worldwide. The optineurin (OPTN) E50K mutation was first identified in familial primary open-angle glaucoma (POAG), the onset of which is not associated with intraocular pressure (IOP) elevation, and is classified as normal-tension glaucoma (NTG). Optineurin (OPTN) is a multifunctional protein and its mutations are associated with neurodegenerative diseases such as POAG and amyotrophic lateral sclerosis (ALS). We have previously described an E50K mutation-carrying transgenic (E50K$^{tg}$) mouse that exhibited glaucomatous phenotypes of decreased retinal ganglion cells (RGCs) and surrounding cell death at normal IOP. Further phenotypic analysis of these mice revealed persistent reactive gliosis and E50K mutant protein deposits in the outer plexiform layer (OPL). Over-expression of E50K in HEK293 cells indicated accumulation of insoluble OPTN in the endoplasmic reticulum (ER). This phenomenon was consistent with the results seen in neurons derived from induced pluripotent stem cells (iPSCs) from E50K mutation-carrying NTG patients. The E50K mutant strongly interacted with TANK-binding kinase 1 (TBK1), which prohibited the proper oligomerization and solubility of OPTN, both of which are important for OPTN intracellular transition. Treatment with a TBK1 inhibitor, BX795, abrogated the aberrant insolubility of the E50K mutant. Here, we delineated the intracellular dynamics of the endogenous E50K mutant protein for the first time and demonstrated how this mutation causes OPTN insolubility, in association with TBK1, to evoke POAG.**

## INTRODUCTION

Glaucoma is one of the world's leading cause of adult-onset blindness that causes optic nerve degeneration characterized by progressive and irreversible loss of retinal ganglion cells (RGCs) and retinal nerve fiber layer defects accompanied by the corresponding visual field damage (1). Open-angle glaucoma, the most prevalent subtype among various glaucomas, is further subdivided into two major types according to intraocular pressure (IOP). In the high-IOP type or primary open-angle glaucoma (POAG), elevated IOP due to disturbance of aqueous humor outflow in the trabecular meshwork or Schlemm's canal mechanically damages RGCs (2). In the normal-IOP type or normal-tension glaucoma (NTG), IOP elevation does not necessarily cause glaucoma, but some IOP-independent factors are thought to be involved (2). According to a population-based glaucoma survey conducted in Japan, NTG is the most prevalent subtype of glaucoma in the country (3, 4). This epidemiological study in Japan reported that the subjects' average IOP was ~15 mmHg and the POAG prevalence was almost equivalent in groups with IOP higher or lower than the average IOP (4). We have investigated the onset mechanism of the latter glaucoma subset, with lower IOP than average, as NTG. Interestingly enough, IOP-unrelated genetic mutations have been found recently in NTG (5, 6) and the Optineurin (OPTN) E50K mutation was the first one identified in familial NTG (7).

OPTN, a scaffold protein with various biological functions, has a few coiled-coil domains and a ubiquitin-binding domain

*To whom correspondence should be addressed at: Division of Molecular and Cellular Biology, National Institute of Sensory Organs, National Hospital Organization Tokyo Medical Center, 2-5-1 Higashigaoka, Meguro-ku, Tokyo 152-8902, Japan. Tel/Fax: +81 334111026; Email: iwatatakeshi@kankakuki.go.jp

at C-terminal. It associates with membrane trafficking proteins Myosin VI and Rab 8 to form Golgi ribbons and is involved in exocytosis (8, 9). And thus E50K mutation yields several phenotypes, such as fragmentation of Golgi apparatus (10), transport failure (8, 11) or apoptotic cell death (12, 13).

OPTN also participates in innate immunity response by regulating NF-κB activation and autophagy in anti-infection processes (14, 15) and via its interaction with some other proteins (16). Among the several OPTN mutations described in the original report, the role of a glutamic acid-to-lysine conversion at amino acid 50 (E50K) in NTG is well accepted worldwide (17–19). A family with a history of NTG was previously identified with the E50K mutation, and in affected members of this family, visual failure starts at about the age of 30 years (Supplementary Material, Fig, S1) and progresses to glaucoma without elevation of IOP until vision is entirely lost at about the age of 70 years (19). Recently, Maruyama *et al.* (20) identified three additional mutations in *OPTN*, a deletion in exon 5, a nonsense mutation (Q398X) and a missense mutation (E478G) that was associated with amyotrophic lateral sclerosis (ALS). Among these three mutations, the former two were recessive mutations and the latter E478G mutation was a dominant mutation, like E50K. The authors further showed the attenuation of the inhibitory effect of NF-κB activation by OPTN carrying the E478G mutation, but that the inhibitory function remained intact with the E50K mutation. Though the underlying causes of OPTN mutation-driven changes are different in POAG and ALS, it is still intriguing that OPTN plays crucial roles in neural homeostasis.

All these results suggest that the E50K mutant expression restricts retinal neural cell survival and is thus involved in the progression of POAG. The underlying molecular mechanism of how the glaucoma phenotype is evoked by a single amino acid replacement in OPTN is still unknown.

In this study, we further characterized the effects of the E50K mutation in OPTN in E50K transgenic ($E50K^{-tg}$) mice and explored the endogenous OPTN dynamics in neural cells differentiated from induced pluripotent stem cells (iPSCs) derived from NTG patients with the genetic mutation corresponding to E50K. At the molecular level, abnormal insolubility of the endogenous E50K OPTN mutant was demonstrated in this study for the first time. This insolubility was simultaneously attributed to the formation of a distinct protein complex, and to disabled oligomerization of OPTN, associated with an enhanced E50K–tank-binding kinase (TBK)1 interaction. The abnormal insolubility of the E50K mutant was rescued by treatment with a TBK1-specific inhibitor.

## RESULTS

### OPTN E50K transgenic mice exhibit profound gliosis in the retina

In our previous report, we showed that $E50K^{-tg}$ mice exhibited phenotypes, such as a decreased number of RGCs and progressive diminution of retinal thickness without elevation of IOP (19). Immunohistochemistry of the flat-mount retinas of $E50K^{-tg}$ mice showed persistent glial fibrillary acidic protein (GFAP)-positive dot-staining between astrocytes, compared with the staining pattern in retinas of wild-type mice (Fig. 1A and B). Evaluation of the pathological condition in age-matched wild-type and mutant mice by pathologists blinded to the sample source indicated significantly increased gliosis in the $E50K^{-tg}$ mice, compared with the wild-type mice (Fig. 1C). GFAP-positive Müller cells are known as one of the hallmarks for retinal neurodegenerative conditions, including glaucoma (21), which can be simulated by various retinal insults such as the optic nerve axonal damage, laser ablation and intravitreal injection of kainic acid (22–24). From the morphological analysis of the cells that appeared in the vertically incised retinal surface (Fig. 1D, dashed line), the GFAP-positive dots shown in the flat-mount specimen were concluded to be Müller cells, from their peculiar spindle shape (Fig. 1D, arrowheads). Reactive gliosis has been reported to be associated with retinal physical insults; thus, this phenotype in $E50K^{-tg}$ mice in the absence of physical insults was of particular interest. Therefore, in addition to the reactive gliosis in the retinas of $E50K^{-tg}$ mice, the retinal vessels were examined by *z*-axis confocal laser microscopy after tail vein injection of red fluorescent dye-conjugated isolectin. The confocal microscopy images revealed a number of gliosis scars embracing leakage of isolectin from vessels (Supplementary Material, Fig. S2A). These findings suggest that the retinas of $E50K^{-tg}$ mice are under continuous stress and are structurally vulnerable.

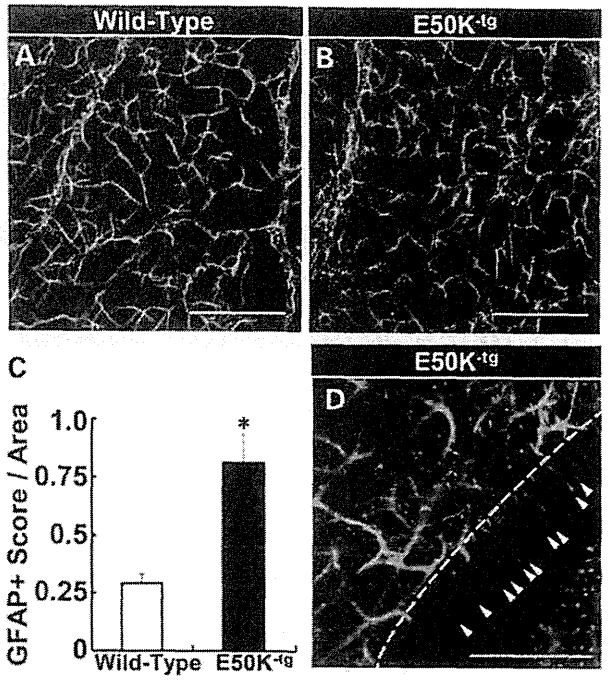


**Figure 1.** Persistent reactive gliosis in E50K-transgenic ($E50K^{-tg}$) mouse retinas. Representative retinal flat-mount immunohistochemistry images of anti-GFAP in (A) wild-type and (B) $E50K^{-tg}$ mice. Scale bar = 200 μm. Flat-mount specimens were analyzed (blinded evaluation) for gliosis assessment. The scores of GFAP-positive gliosis area/retinal area are plotted (data are mean ± SD; four fields of micrographs were chosen randomly and analyzed from one specimen. $n = 4$, $^*P < 0.05$). (D) The appearance of GFAP-positive Müller cells in $E50K^{-tg}$ mice. The dashed line indicates the border of the retinal luminal surface and the incised surface of the retina; arrowheads indicate the feet of GFAP-positive astrocytes. Scale bar = 100 μm. Some of the gliosis harbors the retinal vessel leakage (Supplementary Material, Fig. S1A).

### OPTN E50K protein accumulates in the outer plexiform layer of the retinas of E50K$^{tg}$ mice

Considering the previous report of the deposit-like pathology in motor neurons in the ALS-associated OPTN E478G mutation (20), we also investigated the localization of the OPTN E50K protein in the retinas of E50K$^{tg}$ mice by immunohistochemistry. Negative control slides, treated with rabbit IgG cocktail alone, did not exhibit significant signals (Fig. 2A and B), while the retinas of E50K$^{tg}$ mice exhibited positive staining for OPTN in the outer plexiform layer (OPL) and the inner nuclear layer (INL), as small dot-like deposits (Fig. 2D and F, arrows). The retinas of wild-type littermates did not exhibit such a pattern (Fig. 2C and E). We designed this transgenic mouse with N-terminally HA-tagged OPTN protein, which would enable us to confirm whether the deposits include E50K mutant protein. HA-tagged E50K was mainly detected in the OPL of the retinas in E50K$^{tg}$ mice, which was consistent with the immunostaining results with the anti-OPTN antibody (Supplementary Material, Fig. S3D, arrows). Positive signals were not detected for OPTN in control slides in the retinas of wild-type mice and in those treated with the IgG alone (Supplementary Material, Fig. S3A–C). Thus, OPTN deposits in the retinas of E50K$^{tg}$ mice were caused exclusively from the expression of the E50K mutant. These pathology findings point to the capacity of the E50K mutant protein to aggregate.

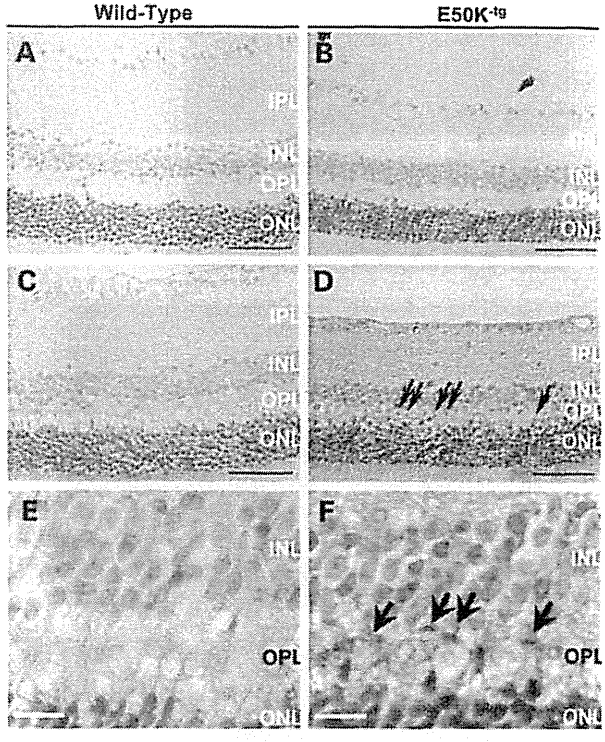


Figure 2. E50K mutant protein deposits in the retinas of E50K$^{tg}$ mice. (**A**) Rabbit IgG negative control for the immunohistochemistry analysis of the retina of a wild-type mouse. (**B**) Rabbit IgG negative control for the immunohistochemistry analysis of the retina of an E50K$^{tg}$ mouse. Both negative control slides showed minimum background staining. (**C**) Anti-OPTN immunohistochemistry of the wild-type mouse retina. Moderate OPTN signals were detected in luminal to inner layers of the retina. (**D**) Anti-OPTN immunohistochemistry of the E50K$^{tg}$ mouse. In addition to the moderate OPTN signals similar to that in the wild-type mouse retina, some strong deposit-like signals from INL to OPL were detected (indicated with arrows). Scale bars = 50 $\mu$m. High magnification micrograph of the retina of (**E**) wild-type and (**F**) E50K$^{tg}$ mice. Arrows indicate the OPTN deposit-like signals. Scale bars = 10 $\mu$m. The OPTN signals consists of, at least to some extent, the E50K$^{tg}$ transgene product, from the results of immunohistochemistry analysis with an anti-HA antibody (Supplementary Material, Fig. S2D). INL, inner nuclear layer; OPL, outer plexiform layer; ONL, outer nuclear layer.

### Examination of induced neural cells from NTG patient-derived iPSCs indicates disturbed OPTN transition from ER to Golgi and Golgi body constriction

To clarify the cause of E50K mutant protein deposits in the retinas of E50K$^{tg}$ mice, we first examined the intracellular localization of wild-type OPTN and the E50K mutant by transfecting vectors encoding the two proteins fused with enhanced green fluorescent protein (EGFP) ($^{EGFP}$-OPTN and $^{EGFP}$-E50K, respectively) into HEK 293 cells. $^{EGFP}$-OPTN could be seen as small puncta widely distributed intracellularly, while $^{EGFP}$-E50K was seen as larger puncta accumulated in the perinuclear region, and the Golgi body in the E50K-expressing cells was fragmented (Supplementary Material, Fig. S4B, arrowheads) as previously reported (10, 20). Since Golgi body formation and its membrane trafficking are associated with the endoplasmic reticulum (ER) (25, 26), ER structure was also examined using an ER detection kit (ER-ID, Enzo). Again, the wild-type OPTN was observed as small puncta dispersed within the cytosol (Fig. 3A), while the larger vesicles of the E50K mutant were accumulated in the perinuclear region surrounded by the ER membrane (Fig. 3B, arrows). To elucidate the intracellular localization of endogenous OPTN, we generated induced pluripotent stem cells (iPSCs) from peripheral blood mononuclear cells isolated from NTG patients with the mutation corresponding to E50K and examined OPTN localization in these cells. The pluripotency of iPSCs was confirmed by immunostaining with antibodies specific for Oct3 and Nanog, pluripotency markers (Supplementary Material, Fig. S5A). Neural induction was conducted as previously reported (27, 28) and neuronal differentiation was confirmed by staining with an antibody specific for Tuj1, a neuronal marker (Supplementary Material, Fig. S5B). iPSC-derived neural cells from NTG patients with the mutation corresponding to E50K were immunostained for OPTN and GM130, as a Golgi body marker, along with ER staining. In the iPSCs with wild-type OPTN, derived from a non-glaucoma subject, OPTN-associated vesicles were dispersed within the cells from ER to Golgi networks, in a pattern identical to that in HEK293 cells over-expressing wild-type OPTN (Fig. 3C). However, in the iPSCs from the NTG patient with the mutation corresponding to E50K, the number of OPTN-associated vesicles was decreased, compared with that in the control iPSCs, with dense aggregation in perinuclear regions and shrinkage of the ER/Golgi body (Fig. 3D). Upon microscopic examination under higher magnification, we found that wild-type OPTN frequently localized on the tips of Golgi ribbons (Fig. 3E), while the E50K OPTN mutant in iPSCs from NTG patients accumulated in the ER and Golgi body (Fig. 3F). Co-localization of wild-type OPTN and the Golgi body was

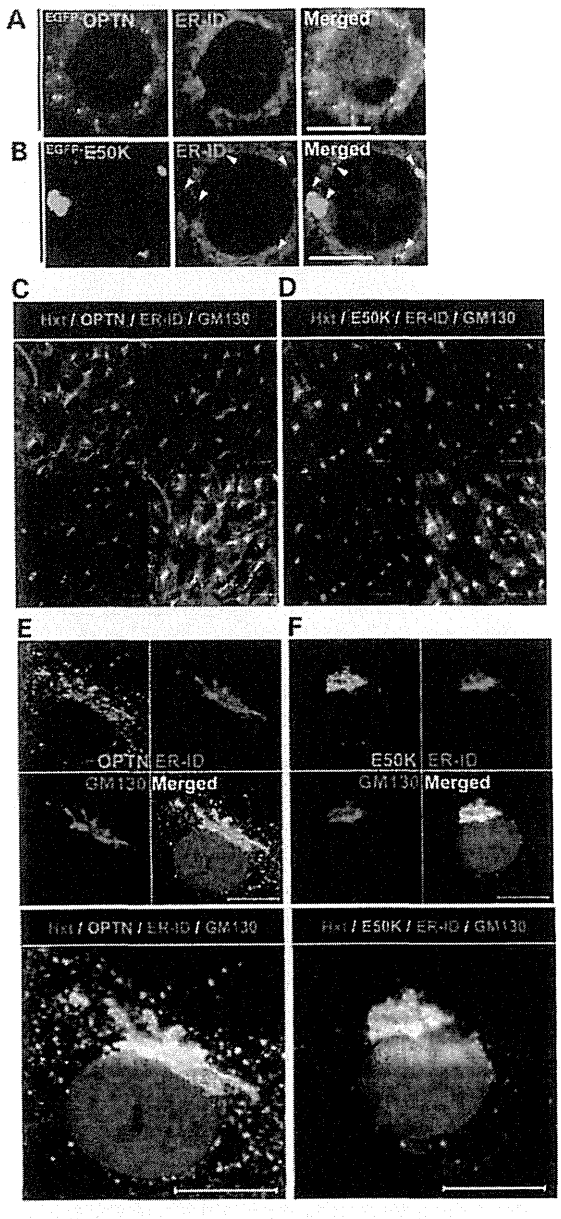


**Figure 3.** Distinct intracellular localization of wild-type OPTN and the E50K mutant. Intracellular localization of OPTN and E50K in over-expression studies. (**A**) $^{EGFP}$-OPTN (green) and ER (red) localization 1 day after transfection. (**B**) $^{EGFP}$-E50K mutant (green) and ER (red) localization 1 day after transfection. Both micrographs are shown with nuclear counter-staining with Hoechst 33342 (blue). Arrowheads indicate the E50K accumulation in the ER. Scale bars = 10 μm. iPSCs were established from iPSCs without the E50K mutation, derived from non-glaucoma subjects, as a control and with the E50K mutation, derived from glaucoma patients for endogenous analyses. Ten days after neural induction, OPTN (green), ER (red) and Golgi (magenta) co-localization were analyzed by immunocytochemistry. (**C**) Endogenous OPTN localization in neural control cells or (**D**) E50K glaucoma patient-derived neural cells. OPTN signals exhibited an accumulated pattern in cells with the E50K mutation. Higher magnification of endogenous OPTN signals in (**E**) control cells and (**F**) cells with the E50K mutation. In control cells, OPTN signals (green vesicles) were localized on the tips of ribbon Golgi body, while in the cells with the E50K mutation, the number of OPTN signals was decreased and largely accumulated within the ER and to a shrunken Golgi body (shown by the white signal in merged micrographs, respectively). All scale bars = 10 μm.

frequently observed (Supplementary Material, Fig. S4A, arrow), but such a co-localization was scarce for the E50K mutant (Supplementary Material, Fig. S4B). These results indicate that the expression of the E50K mutant affects OPTN transition from ER to Golgi body prior to Golgi shrinkage/fragmentation.

### Insolubility of OPTN in iPSCs and iPSC-derived neural cells from NTG patients with the mutation corresponding to E50K

While performing the over-expression experiments, we noticed that the protein amount of over-expressed E50K was decreased to half that of wild-type OPTN in HEK293T cells. A similar result has been previously reported in dermal fibroblasts from the E50K mutation-carrying patients (29). Since there was no significant difference in the mRNA levels in both groups (Supplementary Material, Fig. S6A), we speculated that E50K is more susceptible to intracellular degradation. Our previous studies have shown that OPTN is degraded by proteasomal and lysosomal pathways (30). Therefore, we first treated cells with MG132, a proteasomal inhibitor, and bafilomycin, a lysosomal inhibitor, along with cycloheximide, a protein synthesis inhibitor, to compare the amount of protein degradation. The levels of over-expressed OPTN in cells treated only with cycloheximide were lower, while co-treatment with MG132 or bafilomycin restored the OPTN protein levels, as previously reported (Supplementary Material, Fig. S7A, OPTN lanes). However, over-expressed E50K mutant protein was not restored, unlike over-expressed wild-type OPTN, upon treatment of cells with inhibitors (Supplementary Material, Fig. S7A, E50K lanes). These results indicate that there was no association between the lower levels of the E50K mutant and intracellular degradation of OPTN. We predicted that E50K might be expressed at levels comparable to the wild-type protein, but was probably insoluble and was being precipitated with the insoluble pellet (Ppt.) fraction of the cell lysate after routine cell-lysate collection. Although an equivalent amount of calnexin, a Ppt. marker, was detected in the Ppt. fraction of both wild-type- and E50K-expressing HEK293 cells, ~2- to 5-fold higher amounts of E50K protein, compared with the wild-type OPTN, was detected in the Ppt. fraction (Fig. 4A and B). The insolubilized E50K increased in an E50K expression-dependent manner (Fig. 4C). To elucidate the reason for this altered solubility of E50K mutant protein, we utilized the aforementioned iPSCs and examined the OPTN protein levels by western blotting. Although the OPTN expression was moderate in undifferentiated iPSCs, OPTN was detected in the Sup. fraction of control iPSC lysates (Fig. 4D, control 1–4), while OPTN was detected in the Ppt. fraction of iPSCs from NTG patients with the mutation corresponding to E50K (Fig. 4D, E50K 1–6). OPTN expression was significantly increased after neural induction (Fig. 4E Sup. lanes). The iPSC-derived neural cells recapitulated these results, i.e. abundant OPTN in the Ppt. fraction in E50K mutation-carrying NTG patient-derived cells (Fig. 4E, Ppt. lanes). These findings indicate that regardless of the expression levels, the E50K mutant protein exhibits higher intracellular insolubility.

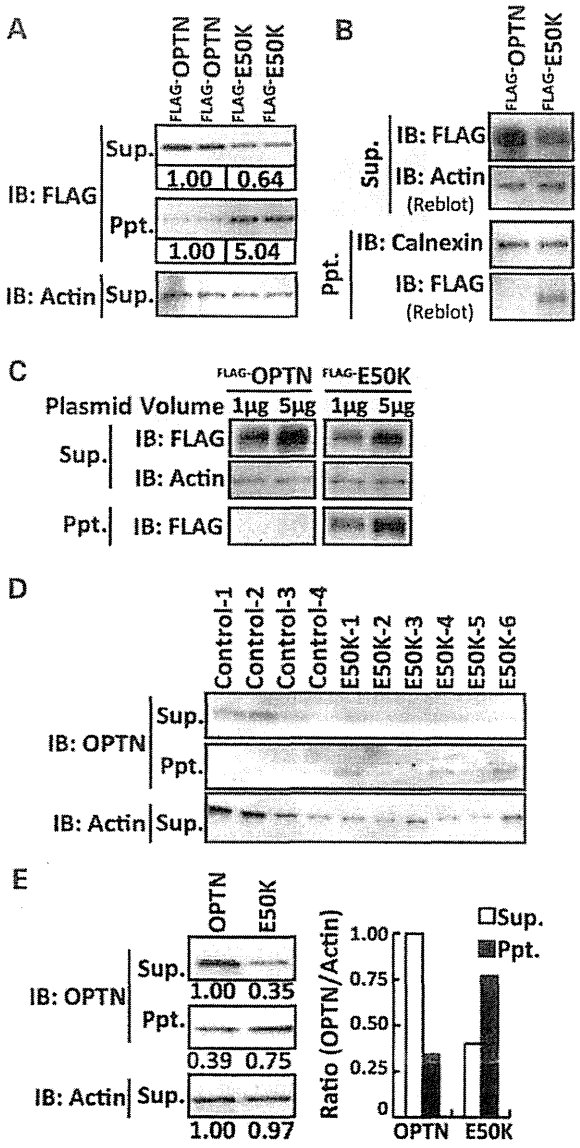


Figure 4. Distinct protein solubility of wild-type OPTN and the E50K mutant. (A) Wild-type OPTN and E50K expression under the same transfection condition. There were no differences in mRNA expressions under these transfection conditions (Supplementary Material, Fig. S4A). The 'Missing' E50K mutant protein was detected in the precipitated fraction (Ppt.), after supernatant (Sup.) collection. Semi-quantitative western blotting analysis was performed using Chemidoc (BioRad) with imaging software and the results are shown under each band. Approximately 2-fold reduction of E50K mutant protein in the Sup. fraction and 2- to 5-fold induction in the Ppt. fraction were observed. (B) Although calnexin, an ER membrane marker, is detected in both the Ppt. fraction of wild-type OPTN-expressing and E50K mutant-expressing cells, only the E50K mutant is detected in the Ppt. fraction. (C) The E50K mutant in the Ppt. fraction was increased in an E50K expression-dependent manner. (D) Endogenous expression and higher hydrophobicity of OPTN in iPSCs with the E50K mutation. Endogenous OPTN is also detected in the Ppt. fraction in iPSCs from E50K mutation-carrying NTG patients. (E) Abundant endogenous expression and higher hydrophobicity of OPTN in iPSC-derived neural cells 10 days after induction from E50K mutation-carrying NTG patients. Semi-quantitative western blotting analysis by Chemidoc with imaging software was performed and the results are shown under each band. The OPTN amounts in each fraction were normalized to the actin amount and then plotted. Sup., supernatant fraction; Ppt., precipitated fraction.

### The enhanced affinity of TBK1 to the E50K mutant protein affects the proper oligomerization and solubility of OPTN

To elucidate the factors that affect the solubility of OPTN, we first examined the native state of wild-type OPTN and the E50K mutant. FLAG-tagged OPTN was expressed in cells and lysates were routinely prepared without detergent and separated by native-polyacrylamide gel electrophoresis (PAGE). Western blotting analysis after native-PAGE indicated more E50K-protein complexes compared with those formed by wild-type OPTN (Fig. 5A). The complexes were immunoprecipitated (IP) using an anti-FLAG antibody and then separated by SDS–PAGE, which revealed distinct binding partners of OPTN and E50K (Fig. 5B, OPTN, white arrowheads; E50K, black arrowheads). We identified each binding partner by liquid chromatography–tandem mass spectrometry (LC–MS/MS). The OPTN partner was identified as OPTN itself, indicating tight oligomerization, while the E50K protein partner was identified as TBK1, which has been previously shown to interact with OPTN by a yeast two-hybrid screening (31). Each candidate interacting partner was further confirmed by IP and western blotting (Fig. 5C and D). Intriguingly, E50K exhibited enhanced affinity to TBK1, while its self-oligomerization was largely decreased (Fig. 5C, arrowhead). Oligomerized OPTN bands clearly seen in wild-type OPTN were restored by treatment with intracellular degradation inhibitors (Supplementary Material, Fig. S7A, left panel, Oligomer lanes), indicating the importance of OPTN oligomerization in intracellular traffic and intracellular degradation. In contrast, these intracellular inhibitors had no effect on the diminished oligomerization of the E50K mutant (Supplementary Material, Fig. S7A right panel, Oligomer lanes). Treatment with a specific inhibitor treatment for TBK1, BX975 (32), was used to examine the relevance of TBK1 binding and the abnormal insolubility of the E50K mutant. BX795 treatment had no effects on the trace amounts of either wild-type OPTN (Supplementary Material, Fig. S7B) or calnexin in the Ppt. fraction (Fig. 5E); on the other hand, the amount of the insolubilized E50K mutant in the Ppt. fraction was drastically decreased by treatment with BX795 in a concentration-dependent manner. Prolonged BX795 treatment was able to restore the E50K mutant protein to the Sup. fraction (Fig. 5F). These findings indicate that the enhanced affinity of E50K for TBK1 is one of the initial pathogenic events that trigger the intracellular insolubility of OPTN leading to improper OPTN transition from the ER to the Golgi body.

## DISCUSSION

The OPTN E50K mutation is the only mutation currently affirmed as causative for NTG, and therefore, it is a clinically relevant mutation for elucidating the mechanism of disease onset at a molecular level (4). Although the E50K mutation is a rare event in familial POAG, the pathology is usually progressive, leading to full blindness even under strict IOP control (Supplementary Material, Fig. S1) (17). Previous reports on E50K mutant phenotypes were focused mainly on *in vitro* models using over-expression studies. Though our initial report on the phenotypic analyses of E50K$^{-tg}$ mice was informative (19), there is a strong necessity for further establishment of the model for OPTN and its target molecules in the endogenous

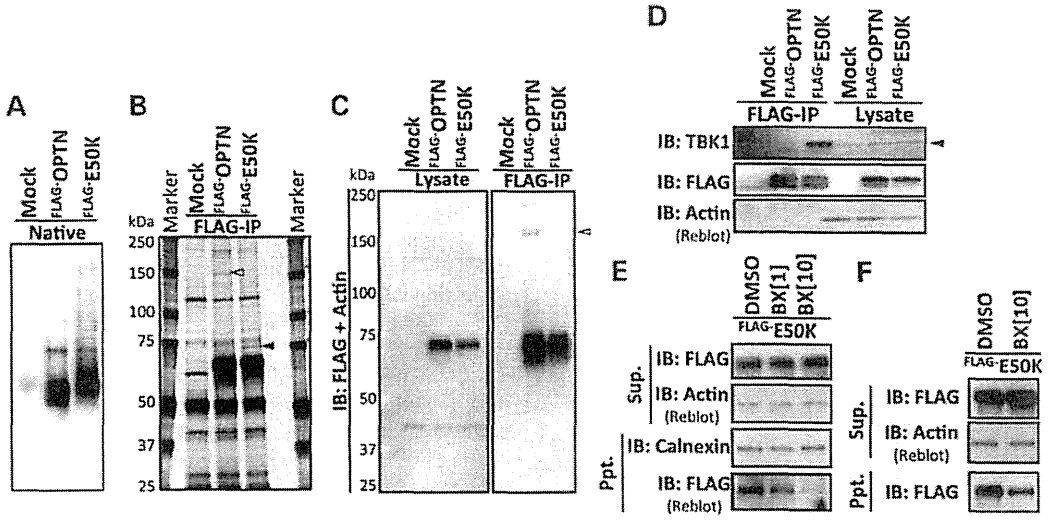


**Figure 5.** Constitutive interaction of the E50K mutant protein and TBK1 evokes the aberrant solubility of OPTN. (**A**) Native-PAGE of mock-transfected controls, wild-type OPTN-transfected cells and E50K-transfected cells revealed the distinct protein complex formation. (**B**) Silver-staining of immunoprecipitates of mock-transfected controls, wild-type OPTN-transfected cells and E50K-transfected cells using an antibody specific for the FLAG-tag. The relevant bands, wild-type OPTN-specific binding molecule (white arrowhead) and E50K mutant-specific binding molecule (black arrowhead), were detected and further analyzed with LC–MS/MS. (**C**) Oligomerization of OPTN. The band indicated with white arrowhead in (B) turned out OPTN itself, i.e. wild-type OPTN is able to oligomerize, while E50K mutant protein largely lacks this oligomerization ability. (**D**) E50K mutant and TBK1 interaction. The band indicated with black arrowhead in (B) turned out TBK1 and E50K mutant protein exhibited higher affinity to TBK1 protein than wild-type OPTN. (**E**) The treatment with BX795, a TBK1 inhibitor, decreases the aberrant precipitation of E50K mutant protein in the Ppt. fraction in a concentration-dependent manner. Dimethylsulfoxide (DMSO) was used as the vehicle control and BX [1], BX [10] indicates the BX795 treatment concentrations of 1 $\mu$g/ml and 10 $\mu$g/ml, respectively, for 3 h. (**F**) Longer treatment with BX795 (6 h with 10 $\mu$g/ml) suppressed aberrant precipitation of E50K mutant protein in the Ppt. fraction and simultaneously restored E50K to the soluble fraction.

context to understand the exact molecular functions of OPTN and its mutations in glaucoma. In addition to the previously identified glaucomatous phenotypes, such as RGC loss, E50K$^{-tg}$ mice also exhibit prominent retinal reactive gliosis with GFAP-positive Müller cells. It has been reported that GFAP-positive Müller cells can be experimentally induced in animal models mimicking glaucomatous phenotypes through various retinal insults, such as axonal damage, intravitreal injection and laser ablation (22–24). Thus, the persistent gliosis and inner layer cell death in E50K$^{-tg}$ mice, without elevation of IOP, were of great interest, and this suggests that increased IOP is not the sole cause for POAG. The deposit-like E50K mutant protein seen in the INL of the retinas of E50K$^{-tg}$ mice was encouraging, because similar abnormal protein inclusions are frequently found in clinical specimens of neurodegenerative tissues, including ALS (20, 33). Why E50K expression, which occurs throughout the body, only affects retinal homeostasis remains unknown. OPTN is also endogenously expressed in many other types of cells, like fibroblasts (7). In addition, most of the other cells expressing OPTN are proliferative and replaced usually within a few months, whereas the neural cells are usually non-proliferative and long-lived. We surmise that this is why the accumulation of E50K over time is critical in the pathogenesis of neurodegenerative diseases, including NTG. Though the E50K$^{-tg}$ mice exhibit some representative neurodegenerative disease phenotypes, further investigation of the E50K accumulation in the endogenous context over time *in vivo* in the retina is needed, preferable in retinal specimens from E50K mutation-carrying NTG patient or from a mouse model, such as a site-specific knock-in mouse model.

Previous *in vitro* studies on E50K have shown large vesicle formation and Golgi fragmentation (10, 20), while there are no reports of endogenous E50K localization and behavior, especially in patient neuronal cells. In general, data pertaining to OPTN in clinical samples of patients with neurodegenerative diseases, including the retinal disease, is scarce. The iPSC technology is one solution to overcome this longstanding limitation by indirectly generating the desired target cells from iPSCs derived from patients with genetically driven neurodegenerative diseases (34). With this first report of the establishment of E50K-glaucoma iPSCs and their neuronal induction, molecular and cellular characterization of POAG onset can now be studied in the endogenous context. iPSC-derived neural cells from E50K mutation-carrying patients revealed for the first time that OPTN accumulated at the constricted Golgi body. In our current experiments, unlike the results of the E50K over-expression studies, Golgi was constricted but not fragmented. This discrepancy should be carefully examined to elucidate whether fragmentation of Golgi body is an endogenous phenotype or just an artifact induced by the over-expression. In any case, excess accumulation of E50K triggers Golgi body deformation and further deteriorates intracellular traffic, and eventually leads to cell death. It is well known that OPTN has a role in secretory vesicle transport and that E50K expression decreases the release of the neurotrophic factor NT3 (9, 35). Furthermore, prostaglandin E2 (PGE2) release via exocytosis is also decreased by E50K expression (Supplementary Material, Fig. S1B). These results indicate that due to the intracellular transport failure in cells expressing the E50K mutant, the paracrine activity for cellular protection and blood flow within the retina would also be attenuated.

Retinal vessel vulnerability in E50K$^{-tg}$ mice is explained by these indirect extracellular E50K effects.

This study demonstrated that the E50K mutant is insoluble and is associated with the hydrophobic precipitate in lysates, compared with the wild-type OPTN, in iPSCs and iPSC-derived neural cells. Abnormal protein deposits, as shown in the retinas of the E50K$^{-tg}$ mice, and protein hydrophobicity are frequently reported in neurodegenerative diseases (36–38). Recent reports in yeast models also supported the distinct hydrophobicities of wild-type OPTN and the E50K mutant (39). Although the prediction of isoelectric points (Compute pI/Mw, ExPASy) of wild-type OPTN and E50K do not differ (OPTN = 5.21, E50K = 5.26), their intracellular protein complex formation is considerably different. The amino acid characteristic of hydrophobic glutamate (E) against hydrophilic lysine (K) suggests that the E50K mutation is a possible charge swap mutation. E50K is located adjacent to the coiled-coil domain, which is a domain implicated in the interaction between OPTN and TBK1 (31, 15). The hydrophobicity of the E50K mutant was closely related with its enhanced interaction with TBK1, a well-known infection-responsive molecule. TBK1 induces macroautophagy by interacting with wild-type OPTN only under conditions of infection, and mediates crosstalk between innate immune response and autophagy (15). Additionally, the copy number variation of *TBK1* was associated with NTG onset (5, 6). The duplication of genes on chromosome 12q14 with familial POAG suggested that an extra copy of the *TBK1* gene and its copy number variation were responsible for NTG (40). More recently, NTG-related TBK1 mutations were also reported (41). Thus it is now well established that both *OPTN* and *TBK1* missense mutations are related with NTG onset. The abnormal physical protein interaction with TBK1 is responsible for the major cause of NTG in relation to the OPTN-E50K mutation. Together with the clinical facts, it has been reported that TBK1 has an important role in innate immunity pathways, and phosphorylated the ER-resident adaptor protein stimulator of IFN genes (STING) to enable IFN production (42, 43). Complexes of these molecules may be involved with the failure of the E50K OPTN protein to transition from ER to Golgi. Although TBK1 contributes to infection-related immunological responses, it also seems to contribute to the intracellular clearance of unnecessary components, such as by autophagy (15). Many other ophthalmic diseases, like macular diseases, are associated with abnormal protein metabolism (44); thus, the crosstalk of OPTN and TBK1 in the maintenance of intracellular clearance in retinal cells is likely to play a significant role in not only glaucomatous but also various other retinal diseases. Even though the exact function of TBK1 and the mechanism of the OPTN-TBK1 crosstalk in retinal homeostasis needs to be elucidated, compounds that abrogate the interaction between the E50K mutant and TBK1 are likely to be beneficial in the treatment of NTG patients.

Our current results pinpoint the molecular basis and concepts of NTG onset in E50K mutation-carrying patients and suggest that the RGC loss, the hallmark of glaucoma, is rather a terminal consequence of the sequential events, i.e. altered affinity of the E50K mutant inhibits self-oligomerization, leading to increased hydrophobicity, which affects downstream functions of OPTN, and eventually leads to cell death. Chronic and excessive accumulation of the E50K mutant protein recapitulated the partial neurodegenerative pathology, including reactive gliosis, vulnerability of retinal vessels and increased apoptotic cell death.

RGC loss is a hallmark of glaucoma; however, the results of this study showed that this phenomenon in E50K-NTG model is at the terminal stage of sequential abnormal events in the retina. In-depth characterization of the mutant protein in a physiologically relevant context and the proper choice/availability of a suitable animal model will help to elucidate and explore therapeutics for personalized treatment of glaucoma in the future.

## MATERIALS AND METHODS

### Antibodies and biochemical analysis

All the antibodies for biochemical studies were purchased from the following companies: anti-OPTN antibody (Cayman); anti-TBK1 antibody (Cell Signaling Technology); anti-FLAG (Sigma); anti-HA (Roche) and anti-Actin (Millipore). The TBK1 inhibitor, BX795, and cycloheximide were purchased from Calbiochem. Mini-PROTEAN TGX Gel and Transblot turbo system (BioRad) were used for native and SDS–PAGE western blotting according to the manufacturer's instructions. Quantitative western blotting was performed with ChemiDoc XRS+ with the Image lab software package (Biorad).

### Animal experiments, preparation of retinal flat-mounts for staining and immunohistochemistry

All animal experiments were carried out in accordance with the Guide for the Care and Use of Laboratory Animals (National Institutes of Health) and the Association for Research in Vision and Ophthalmology Statement for the Use of Animals in Vision Research and approved by the Tokyo Medical Center Experimental Animal Committee. The OPTN mutant E50K$^{-tg}$ mouse used in this study has been described previously (19). Twenty-two to 24-month-old male E50K$^{-tg}$ mice ($n = 4$) and their littermates ($n = 4$) were sacrificed for the assessment of retinal gliosis. Both eyes were dissected and immunostained in flat-mounts as previously described (19). Briefly, dissected eyes were fixed in 2% paraformaldehyde and permeabilized with 0.1% Triton-phosphate-buffered saline (PBS). Non-specific binding was prevented by blocking with DAKO's serum-free blocking buffer, and all specimens were incubated with Alex488-conjugated anti-GFAP antibody (Millipore) for 4°C, over two nights. After radial dissection, retinas were mounted in DAKO's fluorescent mounting medium. A total of 16 retinal specimens, with four micrographs per one retinal specimen, were imaged by LSM700 confocal fluorescence microscopy (Zeiss) using a blinded method. Image analysis was conducted using the ZEN software (Zeiss) and the GFAP-positive area per retinal area was scored. The anti-OPTN (Cayman) and anti-HA (COVANCE) antibodies were used under heated antigen-retrieval conditions. Endogenous peroxidase was quenched by 3% $H_2O_2$ in MeOH. After primary antibody reaction for 4°C overnight, simple rabbit IgG-horse radish peroxidase (HRP) stain and mouse IgG-HRP stain for mouse tissue (Nichirei) were used as secondary HRP-conjugated polymers. After developing with 3,3′-diaminobenzidine (DAB) substrate, specimens were counter-stained with Gill's hematoxylin.

Light microscopy was performed with an Eclipse 600 microscope (Nikon).

### Cell culture, transfection and immunocytochemistry

HEK293T cells were cultured in Dulbecco's modified Eagle medium (DMEM), supplemented with 10% heat-inactivated FBS. The TransIT-PRO Transfection Kit (Mirus) was used according to the manufacturer's instructions. HEK293T cells were transfected with pAC-$^{GFP}$, pAC-$^{GFP}$-OPTN and pAC-$^{GFP}$-E50K to assess the intracellular localization of tagged OPTN. The ER-ID Red assay kit (Enzo) was used for endoplasmic reticulum staining. Anti-GM130 and Alexa633-conjugated anti-mouse IgG antibodies were used for Golgi immunostaining. The following constructs were used for over-expression studies: pEF-BOS-$^{FLAG}$ (45), pEF-BOS-$^{FLAG}$-Optineurin and pEF-BOS-$^{FLAG}$-E50K.

### Generation of iPSC and induction of differentiation to neural cells

Human E50K mutation-carrying iPSCs and the corresponding control iPSCs were established by Sendai-viral (DNAVEC) infection as previously reported (46) from circulating T-cells in the peripheral blood of human familial glaucoma patients with fully informed consent. All procedures were approved by the Ethics Committee of National Hospital Organization Tokyo Medical Center. For maintaining the pluripotency, iPSCs were cultured in bovine fibroblast growth factor (bFGF)-containing iPSC media on Matrigel-coated culture dishes. Oct3 and Nanog were used as pluripotency markers and Tuj1 was used as the neuronal marker. Neural cell induction was performed via embryoid body formation as described previously (27, 28), utilizing the Neuron differentiation Kit (R&D Systems) in accordance with the manufacturer's procedures.

### Identification of E50K-binding proteins by LC–MS/MS

Samples for LC–MS/MS analysis were prepared by preparing lysates from HEK293T cells over-expressing FLAG-tagged OPTN from pEF-BOS-$^{FLAG}$, pEF-BOS-$^{FLAG}$-Optineurin or pEF-BOS-$^{FLAG}$-E50K. Each lysate sample was immunoprecipitated with M2-FLAG-Agarose (Sigma) for 2 h at 4°C. The immunoprecipitated beads were washed with lysis buffer five times and then eluted with 2 M urea. The eluates were electrophoresed on 7.5% SDS–PAGE gels and the gels were silver-stained with the Silver Quest Kit (Invitrogen). The band of interest was processed for in-gel digestion for further LC–MS/MS analysis. Samples were analyzed with LCQ-DECA XP (Thermo Scientific). The obtained binding candidates and their interaction with OPTN/E50K were confirmed by immunoprecipitation and western blotting.

## SUPPLEMENTARY MATERIAL

Supplementary Material is available at HMG online.

## FUNDING

This work was supported by grants to T.I. by the Japanese Ministry of Health, Labour and Welfare (10103254), National Hospital Organization of Japan and the Japan Society for the Promotion of Science (09005752 to T.I., 24791885 to Y.M.). The pEF-BOS vector was a kind gift from Dr Seisuke Hattori in Kitasato University.

## AUTHOR CONTRIBUTIONS

Y.M. and T.I designed the study; Y.M., D.I., H.K., Z.-L.C., H.K., performed the experiments; K.K., T.Y., T.S., S.Y., K.F. contributed new reagents/techniques; Y.M. and T.I. analyzed the data; Y.M. and T.I. wrote the paper.

## REFERENCES

1. Quigley, H.A. and Broman, A.T. (2006) The number of people with glaucoma worldwide in 2010 and 2020. *Br. J. Ophthalmol.*, **90**, 262–267.
2. Quigley, H.A. (2011) Glaucoma. *Lancet*, **377**, 1367–1377.
3. Suzuki, Y., Iwase, A., Araie, M., Yamamoto, T., Abe, H., Shirato, S., Kuwayama, Y., Mishima, H.K., Shimizu, H., Tomita, G. *et al.* (2006) Risk factors for open-angle glaucoma in a Japanese population: the Tajimi Study. *Ophthalmology*, **113**, 1613–1617.
4. Iwase, A., Suzuki, Y., Araie, M., Yamamoto, T., Abe, H., Shirato, S., Kuwayama, Y., Mishima, H.K., Shimizu, H., Tomita, G. *et al.* (2004) The prevalence of primary open-angle glaucoma in Japanese: the Tajimi Study. *Ophthalmology*, **111**, 1641–1648.
5. Fingert, J.H., Robin, A.L., Stone, J.L., Roos, B.R., Davis, L.K., Scheetz, T.E., Bennett, S.R., Wassink, T.H., Kwon, Y.H., Alward, W.L. *et al.* (2011) Copy number variations on chromosome 12q14 in patients with normal tension glaucoma. *Hum. Mol. Genet.*, **20**, 2482–2494.
6. Kawase, K., Allingham, R.R., Meguro, A., Mizuki, N., Roos, B., Solivan-Timpe, F.M., Robin, A.L., Ritch, R. and Fingert, J.H. (2012) Confirmation of TBK1 duplication in normal tension glaucoma. *Exp. Eye Res.*, **96**, 178–180.
7. Rezaie, T., Child, A., Hitchings, R., Brice, G., Miller, L., Coca-Prados, M., Heon, E., Krupin, T., Ritch, R., Kreutzer, D. *et al.* (2002) Adult-onset primary open-angle glaucoma caused by mutations in optineurin. *Science*, **295**, 1077–1079.
8. Sahlender, D.A., Roberts, R.C., Arden, S.D., Spudich, G., Taylor, M.J., Luzio, J.P., Kendrick-Jones, J. and Buss, F. (2005) Optineurin links myosin VI to the Golgi complex and is involved in Golgi organization and exocytosis. *J. Cell Biol.*, **169**, 285–295.
9. Bond, L.M., Peden, A.A., Kendrick-Jones, J., Sellers, J.R. and Buss, F. (2011) Myosin VI and its binding partner optineurin are involved in secretory vesicle fusion at the plasma membrane. *Mol. Biol. Cell*, **22**, 54–65.
10. Park, B.C., Shen, X., Samaraweera, M. and Yue, B.Y. (2006) Studies of optineurin, a glaucoma gene: Golgi fragmentation and cell death from overexpression of wild-type and mutant optineurin in two ocular cell types. *Am. J. Pathol.*, **169**, 1976–1989.
11. Nagabhushana, A., Chalasani, M.L., Jain, N., Radha, V., Rangaraj, N., Balasubramanian, D. and Swarup, G. (2010) Regulation of endocytic trafficking of transferrin receptor by optineurin and its impairment by a glaucoma-associated mutant. *BMC Cell Biol.*, **11**, 4.
12. Chalasani, M.L., Radha, V., Gupta, V., Agarwal, N., Balasubramanian, D. and Swarup, G. (2007) A glaucoma-associated mutant of optineurin selectively induces death of retinal ganglion cells which is inhibited by antioxidants. *Invest. Ophthalmol. Vis. Sci.*, **48**, 1607–1614.
13. Meng, Q., Lv, J., Ge, H., Zhang, L., Xue, F., Zhu, Y. and Liu, P. (2012) Overexpressed mutant optineurin(E50K) induces retinal ganglion cells apoptosis via the mitochondrial pathway. *Mol. Biol. Rep.*, **39**, 5867–5873.
14. Gleason, C.E., Ordureau, A., Gourlay, R., Arthur, J.S. and Cohen, P. (2011) Polyubiquitin binding to optineurin is required for optimal activation of TANK-binding kinase 1 and production of interferon beta. *J. Biol. Chem.*, **286**, 35663–35674.
15. Wild, P., Farhan, H., McEwan, D.G., Wagner, S., Rogov, V.V., Brady, N.R., Richter, B., Korac, J., Waidmann, O., Choudhary, C. *et al.* (2011)

Phosphorylation of the autophagy receptor optineurin restricts Salmonella growth. *Science*, **333**, 228–233.
16. Ying, H. and Yue, B.Y. (2012) Cellular and molecular biology of optineurin. *Int. Rev. Cell. Mol. Biol.*, **294**, 223–258.
17. Aung, T., Rezaie, T., Okada, K., Viswanathan, A.C., Child, A.H., Brice, G., Bhattacharya, S.S., Lehmann, O.J., Sarfarazi, M. and Hitchings, R.A. (2005) Clinical features and course of patients with glaucoma with the E50K mutation in the optineurin gene. *Invest. Ophthalmol. Vis. Sci.*, **46**, 2816–2822.
18. Hauser, M.A., Sena, D.F., Flor, J., Walter, J., Auguste, J., Laroeque-Abramson, K., Graham, F., Delbono, E., Haines, J.L., Pericak-Vance, M.A. *et al.* (2006) Distribution of optineurin sequence variations in an ethnically diverse population of low-tension glaucoma patients from the United States. *J. Glaucoma*, **15**, 358–363.
19. Chi, Z.L., Akahori, M., Obazawa, M., Minami, M., Noda, T., Nakaya, N., Tomarev, S., Kawase, K., Yamamoto, T., Noda, S. *et al.* (2010) Overexpression of optineurin E50K disrupts Rab8 interaction and leads to a progressive retinal degeneration in mice. *Hum. Mol. Genet.*, **19**, 2606–2615.
20. Maruyama, H., Morino, H., Ito, H., Izumi, Y., Kato, H., Watanabe, Y., Kinoshita, Y., Kamada, M., Nodera, H., Suzuki, H. *et al.* (2010) Mutations of optineurin in amyotrophic lateral sclerosis. *Nature*, **465**, 223–226.
21. Ganesh, B.S. and Chintala, S.K. (2011) Inhibition of reactive gliosis attenuates excitotoxicity-mediated death of retinal ganglion cells. *PLoS One*, **6**, e18305.
22. Wurm, A., Iandiev, I., Uhlmann, S., Wiedemann, P., Reichenbach, A., Bringmann, A. and Pannicke, T. (2011) Effects of ischemia-reperfusion on physiological properties of Muller glial cells in the porcine retina. *Invest. Ophthalmol. Vis. Sci.*, **52**, 3360–3367.
23. Giani, A., Thanos, A., Roh, M.I., Connolly, E., Trichonas, G., Kim, I., Gragoudas, E., Vavvas, D. and Miller, J.W. (2011) In vivo evaluation of laser-induced choroidal neovascularization using spectral-domain optical coherence tomography. *Invest. Ophthalmol. Vis. Sci.*, **52**, 3880–3887.
24. Ueda, K., Nakahara, T., Hoshino, M., Mori, A., Sakamoto, K. and Ishii, K. (2010) Retinal blood vessels are damaged in a rat model of NMDA-induced retinal degeneration. *Neurosci. Lett.*, **485**, 55–59.
25. Lasiecka, Z.M. and Winckler, B. (2011) Mechanisms of polarized membrane trafficking in neurons – focusing in on endosomes. *Mol. Cell. Neurosci.*, **48**, 278–287.
26. Farhan, H., Freissmuth, M. and Sitte, H.H. (2006) Oligomerization of neurotransmitter transporters: a ticket from the endoplasmic reticulum to the plasma membrane. *Handb. Exp. Pharmacol.*, **175**, 233–249.
27. Tsuji, O., Miura, K., Okada, Y., Fujiyoshi, K., Mukaino, M., Nagoshi, N., Kitamura, K., Kumagai, G., Nishino, M., Tomisato, S. *et al.* (2010) Therapeutic potential of appropriately evaluated safe-induced pluripotent stem cells for spinal cord injury. *Proc. Natl Acad. Sci. USA*, **107**, 12704–12709.
28. Tucker, B.A., Scheetz, T.E., Mullins, R.F., DeLuca, A.P., Hoffmann, J.M., Johnston, R.M., Jacobson, S.G., Sheffield, V.C. and Stone, E.M. (2011) Exome sequencing and analysis of induced pluripotent stem cells identify the cilia-related gene male germ cell-associated kinase (MAK) as a cause of retinitis pigmentosa. *Proc. Natl Acad. Sci. USA*, **108**, E569–576.
29. Sarfarazi, M. and Rezaie, T. (2003) Optineurin in primary open angle glaucoma. *Ophthalmol. Clin. North Am.*, **16**, 529–541.
30. Shen, X., Ying, H., Qiu, Y., Park, J.S., Shyam, R., Chi, Z.L., Iwata, T. and Yue, B.Y. (2011) Processing of optineurin in neuronal cells. *J. Biol. Chem.*, **286**, 3618–3629.
31. Morton, S., Hesson, L., Peggie, M. and Cohen, P. (2008) Enhanced binding of TBK1 by an optineurin mutant that causes a familial form of primary open angle glaucoma. *FEBS Lett.*, **582**, 997–1002.
32. Clark, K., Plater, L., Peggie, M. and Cohen, P. (2009) Use of the pharmacological inhibitor BX795 to study the regulation and physiological roles of TBK1 and IkappaB kinase epsilon: a distinct upstream kinase mediates Ser-172 phosphorylation and activation. *J. Biol. Chem.*, **284**, 14136–14146.
33. Ito, H., Nakamura, M., Komure, O., Ayaki, T., Wate, R., Maruyama, H., Nakamura, Y., Fujita, K., Kaneko, S., Okamoto, Y. *et al.* (2011) Clinicopathologic study on an ALS family with a heterozygous E478G optineurin mutation. *Acta Neuropathol.*, **122**, 223–229.
34. Imaizumi, Y., Okada, Y., Akamatsu, W., Koike, M., Kuzumaki, N., Hayakawa, H., Nihira, T., Kobayashi, T., Ohyama, M., Sato, S. *et al.* (2012) Mitochondrial dysfunction associated with increased oxidative stress and alpha-synuclein accumulation in PARK2 iPSC-derived neurons and postmortem brain tissue. *Mol. Brain*, **5**, 35.
35. Sippl, C., Bosserhoff, A.K., Fischer, D. and Tamm, E.R. (2011) Depletion of optineurin in RGC-5 cells derived from retinal neurons causes apoptosis and reduces the secretion of neurotrophins. *Exp. Eye Res.*, **93**, 669–680.
36. Nukina, N., Kosik, K.S. and Selkoe, D.J. (1987) Recognition of Alzheimer paired helical filaments by monoclonal neurofilament antibodies is due to crossreaction with tau protein. *Proc. Natl Acad. Sci. USA*, **84**, 3415–3419.
37. Hoffner, G., Kahlem, P. and Djian, P. (2002) Perinuclear localization of huntingtin as a consequence of its binding to microtubules through an interaction with beta-tubulin: relevance to Huntington's disease. *J. Cell Sci.*, **115**, 941–948.
38. LaVoie, M.J., Ostaszewski, B.L., Weihofen, A., Schlossmacher, M.G. and Selkoe, D.J. (2005) Dopamine covalently modifies and functionally inactivates parkin. *Nat. Med.*, **11**, 1214–1221.
39. Kryndushkin, D., Ihrke, G., Piermartiri, T.C. and Shewmaker, F. (2012) A yeast model of optineurin proteinopathy reveals a unique aggregation pattern associated with cellular toxicity. *Mol. Microbiol.*, **86**, 1531–1547.
40. Fingert, J.H., Darbro, B.W., Qian, Q., Van Rheeden, R., Miller, K., Riker, M., Solivan-Timpe, F., Roos, B.R., Robin, A.L. and Mullins, R.F. (2013) TBK1 and flanking genes in human retina. *Ophthalmic Genet.*, doi:10.3109/13816810.2013.768674.
41. Seo, S., Solivan-Timpe, F., Roos, B.R., Robin, A.L., Stone, E.M., Kwon, Y.H., Alward, W.L. and Fingert, J.H. (2013) Identification of proteins that interact with TANK binding kinase 1 and testing for mutations associated with glaucoma. *Curr. Eye Res.*, **38**, 310–315.
42. Saitoh, T., Fujita, N., Hayashi, T., Takahara, K., Satoh, T., Lee, H., Matsunaga, K., Kageyama, S., Omori, H., Noda, T. *et al.* (2009) Atg9a controls dsDNA-driven dynamic translocation of STING and the innate immune response. *Proc. Natl Acad. Sci. USA*, **106**, 20842–20846.
43. Tanaka, Y. and Chen, Z.J. (2012) STING specifies IRF3 phosphorylation by TBK1 in the cytosolic DNA signaling pathway. *Sci. Signal.*, **5**, ra20.
44. Shaw, P.X., Zhang, L., Zhang, M., Du, H., Zhao, L., Lee, C., Grob, S., Lim, S.L., Hughes, G., Lee, J. *et al.* (2012) Complement factor H genotypes impact risk of age-related macular degeneration by interaction with oxidized phospholipids. *Proc. Natl Acad. Sci. USA*, **109**, 13757–13762.
45. Mizushima, S. and Nagata, S. (1990) pEF-BOS, a powerful mammalian expression vector. *Nucleic Acids Res.*, **18**, 5322.
46. Seki, T., Yuasa, S., Oda, M., Egashira, T., Yae, K., Kusumoto, D., Nakata, H., Tohyama, S., Hashimoto, H., Kodaira, M. *et al.* (2010) Generation of induced pluripotent stem cells from human terminally differentiated circulating T cells. *Cell Stem Cell*, **7**, 11–14.

# CLINICAL CHARACTERISTICS OF OCCULT MACULAR DYSTROPHY IN FAMILY WITH MUTATION OF *RP1L1* GENE

KAZUSHIGE TSUNODA, MD, PHD,* TOMOAKI USUI, MD, PHD,†‡ TETSUHISA HATASE, MD, PHD,† SATOSHI YAMAI, MD,§ KAORU FUJINAMI, MD,* GEN HANAZONO, MD, PHD,* KEI SHINODA, MD, PHD,*¶ HISAO OHDE, MD, PHD,** MASAKAZU AKAHORI, PHD,* TAKESHI IWATA, PHD,* YOZO MIYAKE, MD, PHD*††

**Purpose:** To report the clinical characteristics of occult macular dystrophy (OMD) in members of one family with a mutation of the *RP1L1* gene.

**Methods:** Fourteen members with a p.Arg45Trp mutation in the *RP1L1* gene were examined. The visual acuity, visual fields, fundus photographs, fluorescein angiograms, full-field electroretinograms, multifocal electroretinograms, and optical coherence tomographic images were examined. The clinical symptoms and signs and course of the disease were documented.

**Results:** All the members with the *RP1L1* mutation except one woman had ocular symptoms and signs of OMD. The fundus was normal in all the patients during the entire follow-up period except in one patient with diabetic retinopathy. Optical coherence tomography detected the early morphologic abnormalities both in the photoreceptor inner/outer segment line and cone outer segment tip line. However, the multifocal electroretinograms were more reliable in detecting minimal macular dysfunction at an early stage of OMD.

**Conclusion:** The abnormalities in the multifocal electroretinograms and optical coherence tomography observed in the OMD patients of different durations strongly support the contribution of *RP1L1* mutation to the presence of this disease.

RETINA 32:1135–1147, 2012

Occult macular dystrophy (OMD) was first described by Miyake et al[1] to be a hereditary macular dystrophy without visible fundus abnormalities. Patients with OMD are characterized by a progressive decrease of visual acuity with normal-appearing fundus and normal fluorescein angiograms (FA). The important signs of OMD are normal full-field electroretinograms (ERGs) but abnormal focal macular ERGs and multifocal electroretinograms (mfERGs) also exist. These findings indicated that the retinal dysfunction was confined to the macula.[1–5] Optical coherence tomography (OCT) showed structural changes in the outer nuclear and photoreceptor layers.[6–11]

Recently, we found that dominant mutations in the *RP1L1* gene were responsible for OMD.[12] The *RP1L1* gene was originally cloned as a gene derived from common ancestors as a retinitis pigmentosa 1 (*RP1*) gene, which is responsible for 5–10% of autosomal dominant retinitis pigmentosa worldwide, on the same Chromosome 8.[13–17] A number of attempts have been made to identify mutations in *RP1L1* in various retinitis pigmentosa patients with no success. An immunohistochemical study on cynomolgus monkeys showed that *RP1L1* was expressed in rod and cone photoreceptors, and *RP1L1* is thought to play important roles in the morphogenesis of the photoreceptors.[13,18] Heterozygous *RP1L1* knockout mice were reported to be normal, whereas homozygous knockout mice develop subtle retinal degeneration.[18] However, the RP1L1 protein has a very low degree of overall sequence

From the *Laboratory of Visual Physiology, National Institute of Sensory Organs, Tokyo, Japan; †Division of Ophthalmology and Visual Science, Graduate School of Medical and Dental Sciences, Niigata University, Niigata, Japan; ‡Akiba Eye Clinic, Niigata, Japan; §Department of Ophthalmology, Sado General Hospital, Niigata, Japan; ¶Department of Ophthalmology, School of Medicine, Teikyo University, Tokyo, Japan; **Department of Ophthalmology, School of Medicine, Keio University, Tokyo, Japan; and ††Aichi Medical University, Aichi, Japan.

The authors have no financial interest or conflicts of interest.

Supported in part by research grants from the Ministry of Health, Labor and Welfare, Japan and Japan Society for the Promotion of Science, Japan.

Reprint requests: Kazushige Tsunoda, Laboratory of Visual Physiology, National Institute of Sensory Organs, 2-5-1 Higashigaoka, Meguro-ku, Tokyo 152-8902, Japan; e-mail: tsunodakazushige@kankakuki.go.jp